Systematic study of electric quadrupole excitations in the stable even mass Sn nuclei

J. Bryssinck,[1] L. Govor,[2] V. Yu. Ponomarev,[1,*] F. Bauwens,[1] O. Beck,[3] D. Belic,[3] P. von Brentano,[4] D. De Frenne,[1] T. Eckert,[3] C. Fransen,[4] K. Govaert,[1] R.-D. Herzberg,[4,†] E. Jacobs,[1] U. Kneissl,[3] H. Maser,[3] A. Nord,[3] N. Pietralla,[4] H. H. Pitz,[3] and V. Werner[4]

[1]*Vakgroep Subatomaire en Stralingsfysica, University Gent, Proeftuinstraat 86, 9000 Gent, Belgium*

[2]*Russian Scientific Centre ''Kurchatov Institute,'' Moscow, Russia*

[3]*Institut für Strahlenphysik, Universität Stuttgart, Stuttgart, Germany*

[4]*Institut für Kernphysik, Universität zu Köln, Köln, Germany*

(Received 11 August 1999; published 18 January 2000)

The spherical semimagic ^{116,118,120,122,124}Sn nuclei have been investigated intensively using nuclear resonance fluorescence techniques. The measurement of the photon scattering cross sections, angular distributions, and linear polarization or azimuthal asymmetries of the resonantly scattered (unpolarized and polarized) photons enabled a model independent determination of reduced transition probabilities, level spins, and parities. Besides the enhanced dipole excitations to the well-known $(2_1^+ \otimes 3_1^-)_{1^-}$ two-phonon states several electric quadrupole transitions were detected in the investigated energy region below 4 MeV. Quasiparticle phonon model calculations reveal several collective and noncollective 2^+ states in this energy region. In contrast to the known two-phonon $(2_1^+ \otimes 3_1^-)_{1^-}$ states, the wave functions of the observed 2^+ states are dominated by one-phonon components. However, the fragmentation of the $B(E2)\uparrow$ strength is influenced by two-phonon 2^+ admixtures.

PACS number(s): 23.20.Lv, 21.10.Re, 25.20.Dc, 27.60.+j

I. INTRODUCTION

During the last decade, much experimental and theoretical interest went into the study of low angular momenta (dipole and quadrupole) excitations. The even semimagic Sn nuclei represent an ideal case to investigate in a systematic way the two-phonon $(2_1^+ \otimes 3_1^-)_{1^-}$ state and low-lying 2^+ states. The Sn nuclei, having a spherical shape with small deformation parameters [1,2], form the longest chain of stable isotopes with reasonable abundances in order to get isotopically enriched targets of a few grams. We have investigated the ^{116,118,120,122,124}Sn nuclei in the energy region up to 4 MeV using the nuclear resonance fluorescence (NRF) technique. The low-energy level scheme of spherical nuclei is characterized by strong collective vibrational quadrupole (2_1^+) and octupole (3_1^-) excitations which can be described in a theoretical approach as phonons [3]. The NRF technique is an outstanding tool to investigate the 1^- member of the quadrupole-octupole coupled $(2_1^+ \otimes 3_1^-)_{1^-}$ two-phonon quintuplet [4]. The real photon probe is extremely selective: only dipole and to a lesser extent electric quadrupole transitions are induced and the enhanced electric dipole transitions to the 1^- states correspond with high photon scattering cross sections. Since in the present experiment, the scattering intensities for electric quadrupole transitions are about one order of magnitude weaker than the electric dipole ones, the NRF method allows us to study collective and weakly collective 2^+ excitations with a one-phonon nature. This was demonstrated recently by the investigation of the mixed-symmetry one-phonon 2^+_{ms} state in ^{136}Ba [5] and ^{94}Mo [6]. The observation of two-phonon 2^+ states in NRF experiments is not expected. The $1p$-$1h$ $E2$ strength in the low energy region is nearly totally concentrated in the well-known collective quadrupole 2_1^+ vibration. The remaining $B(E2)\uparrow$ strength is distributed over several other noncollective and weakly collective 2^+ configurations of $1p$-$1h$ nature [7].

Our results on ^{116,124}Sn and the uniform properties of the observed two-phonon $(2_1^+ \otimes 3_1^-)_{1^-}$ states in the Sn isotopes are described in previous papers [8,9]. In the actual paper, we will focus on the full systematics of quadrupole excitations in the five investigated even mass Sn isotopes and on a detailed multiphonon analysis performed within the framework of the quasiparticle phonon model (QPM). The complete experimentally observed data on dipole and electric quadrupole transitions for the ^{116,118,120,122,124}Sn nuclei will be presented and compared with the earlier $(n,n'\gamma)$ data [10].

II. EXPERIMENTAL METHOD AND SETUP

The nuclear resonance fluorescence technique has already been extensively described, see, e.g., Ref. [11]. The experiments reported on here, were performed at the bremsstrahlung NRF facility at the 4.3 MV Dynamitron accelerator of the Stuttgart University [11]. The electron energy was 4.1 MeV. Due to the high quality of the γ beam, two NRF setups are operated simultaneously. A first setup, intended for angular distribution measurements, consists of three coaxial HP Ge detectors at scattering angles of 90°, 127°, and 150° with an efficiency ϵ of 100, 100, and 22 % relative to a 3 in.$\times$3 in. NaI(Tl) scintillation detector. At the second setup, downwards the photon beam, an arrangement with two Compton

*Permanent address: Bogoliubov Laboratory of Theoretical Physics, Joint Institute of Nuclear Research, Dubna, Russia.

†Present address: Oliver Lodge Laboratory, University of Liverpool, Oxford Street, Liverpool L69 7ZE, UK.

polarimeters ($\epsilon \cong$ 60% and 25%) and an additional HP Ge γ detector ($\epsilon \cong$ 38%, at 127°) was installed. The two Compton polarimeters were placed at scattering angles 90° and 95°. The Compton polarimeter with the lower efficiency was surrounded by an active BGO anti-Compton shield in order to improve the response function [12]. Both Compton polarimeters have similar polarization sensitivities Q of about 20% at 0.5 MeV and 9.5% at 4.4 MeV [13]. As the electrical signal from the core of the Compton polarimeter carries the full energy information of the detected γ-rays, angular distribution as well as linear polarization measurements could therefore be carried out with the same setup.

The targets consisted of sandwiched ^{27}Al and isotopically enriched Sn disks with a diameter of 20 mm. The continuous high intensity γ beam enables count rates in the order of 4000 counts per second with an excellent energy resolution and reduces irradiation times to about a few days at the first setup. At this setup, angular distribution measurements on ^{116}Sn, ^{120}Sn, ^{122}Sn, and ^{124}Sn were performed. For ^{118}Sn and ^{122}Sn angular distribution measurements and measurements of the linear polarization of the resonantly scattered photons with Compton polarimetry were carried out at the second setup. The parities of some observed levels in ^{116}Sn and ^{124}Sn nuclei were previously determined via $(\vec{\gamma},\gamma')$ measurements at the NRF setup in Gent [8]. For a detailed description of this setup, we refer to Ref. [14].

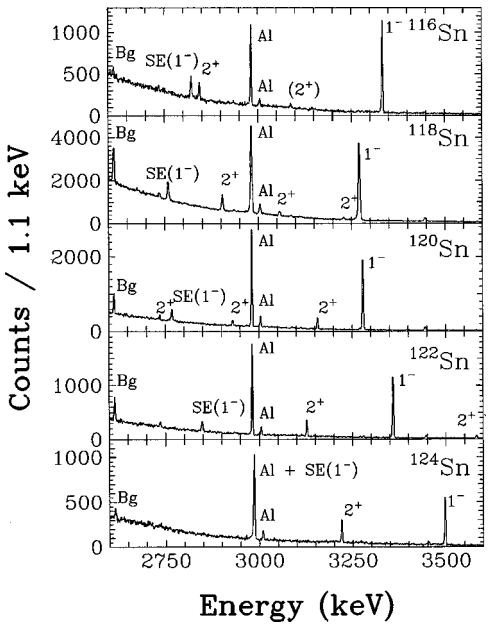

FIG. 1. High energy part (2600 – 3600 keV) of the NRF spectra for ^{116,118,120,122,124}Sn. The dominating peak in each spectrum corresponds to the deexcitation of the $(2_1^+ \otimes 3_1^-)_{1^-}$ state. This peak is indicated with 1^- and its single escape peak with SE(1^-). Prominent 2^+ states are marked with ''2^+.'' The 2614 keV background line from the decay of ^{208}Tl is labeled with ''Bg.'' Lines stemming from the ^{27}Al calibration standard are labeled by ''Al.''

III. EXPERIMENTAL RESULTS

The high energy part of the recorded (γ,γ') spectra on ^{116,118,120,122,124}Sn is shown in Fig. 1. Each spectrum is dominated by the ground state transition from the $(2_1^+ \otimes 3_1^-)_{1^-}$ two-phonon state. Comparison of the expected ratios of the angular distribution functions $W(90°)/W(127°)$ for 0-1-0 and 0-2-0 spin sequences (corrected for the solid angles of the detectors) with the experimentally measured ratios, allowed the identification of several dipole and quadrupole transitions. All the transitions, except the strong $E1$ transitions to the two-phonon states (see Ref. [9]) were too weak to allow any conclusion about the parity in the Compton polarimetry measurements. Nevertheless, observed $J=2$ states should have a positive parity, since $M2$ excitations are known to have scattering intensities below the sensitivity of the setup.

Our experimental results for ^{116,118,120,122,124}Sn are summarized in Table I. Energies are corrected for recoil and, if possible, a weighted average of the results was taken for the scattering angles 90° and 127°. In general, the excitation energies are measured to a precision better than 1 keV. In columns 2 and 3, the spins deduced from the present experiments are compared with the results of the $(n,n'\gamma)$ experiment [10]. No contradiction is found. In ^{118}Sn a new level at 3982 keV and in ^{122}Sn a new level at 3871 keV were observed. In the last two columns the reduced excitation probabilities $B(E1)\uparrow$ and $B(E2)\uparrow$ are given according to the observed spin sequence, the parity of the excited level and the known branching ratios Γ_0/Γ. If the spin could not be determined in this work, it was adopted from the earlier $(n,n'\gamma)$ work [10]. Branching ratios were not observed in our NRF experiments, therefore Γ_0/Γ values are taken from the literature, mainly from recent $(n,n'\gamma)$ investigations [15–19]. In the case of ^{116}Sn, the adopted decay branching for the 2843.9 keV level in Nuclear Data Sheets [20] is not in agreement with data from (n,γ) work [21], from ^{116}Sb (15.8 min) EC decay studies [22] (although the data from both works were included in this issue of the Nuclear Data Sheets) and from $(n,n'\gamma)$ work [15]. The results from Ref. [15] are in very good agreement with the data from the (n,γ) experiment with exception of the 4013 keV level. For this level the data from Ref. [21] were taken.

In columns 7 and 8, the ground state decay widths Γ_0 deduced from our experiments are compared with the ones derived from lifetime τ measurements [10]. The ground state decay widths $\Gamma_{0,(\gamma,\gamma')}$ obtained in (γ,γ') experiments may be smaller than the decay widths $\Gamma_{0,(n,n'\gamma)}$ found in the $(n,n'\gamma)$ measurements. This can be understood from the equations used in the analysis. In NRF, the scattering intensity is proportional to Γ_0^2/Γ whereas in $(n,n'\gamma)$ experiments the lifetime τ is measured:

$$\Gamma_{0,(\gamma,\gamma')} = \frac{\Gamma_0^2}{\Gamma}\frac{\Gamma}{\Gamma_0},$$

$$\Gamma_{0,(n,n'\gamma)} = \frac{\hbar}{\tau}\frac{\Gamma_0}{\Gamma}.$$

If the branching ratio Γ_0/Γ is overestimated due to unobserved transitions to lower-lying excited states $\Gamma_{0,(\gamma,\gamma')}$ will

TABLE I. Properties of the levels observed in ^{116}Sn, ^{118}Sn, ^{120}Sn, ^{122}Sn, and ^{124}Sn.

Energy (keV)	J^π (γ,γ')	J^π [a] $(n,n'\gamma)$	I_S (eV b)	Γ_0^2/Γ (meV)	Γ_0/Γ [b]	$\Gamma_{0,(\gamma,\gamma')}$ (meV)	$\Gamma_{0,(n,n'\gamma)}$ (meV)	$B(E1)\uparrow$ $(10^{-3}e^2\ \mathrm{fm}^2)$	$B(E2)\uparrow$ $(e^2\ \mathrm{fm}^4)$
					^{116}Sn				
1293.6 (3)	2_1^+	2_1^+	12.6 (12)	1.10 (10)	1	1.10 (10)			1883 (171)
2843.9 (3)	2^+	2^+	5.6 (6)	2.37 (26)	0.745 (19)	3.18 (36)	$4.05^{+0.71}_{-0.76}$		106 (12)
3088.7 (6)	(2^+)	2^+	2.2 (4)	1.11 (21)	0.654 (14)	1.70 (32)	$1.43^{+0.83}_{-0.76}$		37 (7)
3333.7 (3)	1^-	$1^{(+)}$	87.8 (87)	84.7 (84)	1	84.7 (84)	51^{+15}_{-12}	6.55 (65)	
4012.9 (6)	1	1	6.1 (26)	8.5 (36)	0.714 (89) [c]	11.9 (53)	16^{+11}_{-6}	0.53 (27)	
4026.8 (5)	1	1	10.4 (40)	14.6 (56)	1	14.6 (56)	<27	0.64 (25)	
					^{118}Sn				
1229.6 (4)	2_1^+	2_1^+	11.8 (16)	0.93 (13)	1	0.93 (13)			2051 (286)
2903.8 (6)	2^+	2^+	5.8 (5)	2.54 (22)	0.730 (19)	3.47 (31)	$4.33^{+0.89}_{-0.90}$		105 (13)
3057.0 (5)		2^+	2.3 (3)	1.12 (13)	0.815 (14)	1.37 (16)	$3.35^{+0.65}_{-1.26}$		32 (4)
3228.2 (6)	(2^+)	2^+	1.5 (3)	0.79 (16)	1	0.79 (16)	$2.99^{+0.45}_{-1.84}$		14 (3)
3270.3 (5)	1^-	1	95.4 (71)	88.5 (65)	1	88.5 (65)	94^{+67}_{-54}	7.25 (54)	
3856.9 (10)	1	$1,2^+$	2.3 (4)	2.98 (57)	0.543 (55)	5.5 (12)		0.27(6)	
3982.2 (8)	1		4.5 (8)	6.2 (11)		6.2 (11)		0.28 (5)	
					^{120}Sn				
1171.2 (6)	2_1^+	2_1^+	12.6 (15)	0.90 (11)	1	0.90 (11)			2521 (299)
2728.9 (11)		2^+	1.5 (6)	0.58 (23)	0.441 (25)	1.32 (52)	$0.83^{+0.38}_{-0.31}$		54 (21)
2930.2 (6)	2^+	2^+	3.9 (5)	1.76 (21)	0.649 (25)	2.71 (35)	$3.29^{+0.99}_{-1.04}$		78 (10)
3157.6 (5)	2^+	2^+	8.4 (8)	4.36 (39)	0.825 (16)	5.29 (49)	$7.5^{+1.8}_{-1.6}$		104 (10)
3278.8 (6)	$1^{(-)}$	1	100.2 (67)	93.4 (63)	1	93.5 (63)	39^{+16}_{-10}	7.60 (51)	
3284.9 (8)		2^+	0.6 (2)	0.31 (11)	0.630 (25)	0.50 (17)	$1.7^{+1.5}_{-1.3}$		8 (3)
3582.5 (7)		2^+	0.8 (2)	0.56 (15)	0.611 (50)	0.91 (26)	$5.0^{+5.0}_{-2.7}$		10 (3)
3764.6 (15)	1	1	2.2 (4)	2.71 (51)	0.529 (42)	5.13 (96)		0.28 (5)	
3835.6 (10)		2^+	1.1 (4)	0.86 (31)	0.489 (40)	1.77 (65)	$1.8^{+2.2}_{-1.5}$		13 (5)
4006.4 (9)		2^+	3.2 (8)	2.70 (77)	1	2.70 (77)			16 (5)
					^{122}Sn				
1140.8 (8)	2_1^+	2_1^+	10.7 (15)	0.73 (10)	1	0.73 (10)			2328 (333)
2415.5 (9)		2^+	1.7 (4)	0.50 (11)	0.706 (22)	0.71 (16)	$0.97^{+0.25}_{-0.23}$		54 (12)
3127.6 (7)	2^+	2^+	11.2 (10)	5.70 (52)	1	5.70 (52)	$10.6^{+2.3}_{-2.1}$		118 (11)
3358.5 (8)	1^-	1	96.7 (72)	94.6 (71)	1	94.6 (71)	73^{+59}_{-26}	7.16 (54)	
3582.5 (8)	2^+	2^+	4.3 (6)	2.89 (38)	0.813 (23)	3.56 (48)	$13.4^{+7.2}_{-5.0}$		30 (4)
3751.5 (11)		2^+	1.6 (4)	1.16 (30)	1	1.16 (30)	$8.2^{+8.2}_{-4.6}$		10 (2)
3759.2 (12)	1	1	2.4 (5)	2.90 (62)	0.344 (34)	8.4 (18)	$5.7^{+17.0}_{-3.4}$	0.46 (10)	
3819.7 (16)		2^+	1.0 (3)	0.76 (24)	0.475 (39)	1.60 (52)	$4.5^{+3.4}_{-2.5}$		12 (4)
3871.0 (9)	1		2.1 (5)	2.72 (64)		2.72 (64)		0.13 (3)	
3929.9 (11)		$1,2^+$	1.9 (6)	1.52 (44)	0.812 (53)	1.88 (55)		0.089 (26)	12 (4)
					^{124}Sn				
1131.8 (4)	2_1^+	2_1^+	7.3 (10)	0.49 (7)	1	0.49 (7)			1629 (224)
2426.5 (5)	(2^+)	2^+	1.3 (3)	2.1 (11)	0.654 (45)	0.63 (16)	$0.85^{+0.32}_{-0.31}$		46 (12)
3214.8 (4)	2^+	2^+	16.5 (18)	8.87 (97)	0.852 (23)	10.4 (12)	$15.6^{+4.5}_{-3.1}$		188 (21)
3490.1 (3)	1^-	1	85.4 (93)	90.2 (98)	1	90.2 (98)	73^{+91}_{-29}	6.08 (66)	
3697.4 (5)	1	$1\ (2^+)$	9.5 (14)	11.3 (17)	0.855 (40)	13.2 (21)	$13.4^{+6.7}_{-4.2}$	0.75 (12)	
3710.5 (5)	(2^+)	2^+	9.2 (14)	6.6 (10)	0.775 (40)	8.5 (14)	$11.9^{+11.3}_{-2.2}$		75 (12)

[a] See Ref. [10].

[b] See for ^{116}Sn Ref. [15], ^{118}Sn Ref. [16], for ^{120}Sn Ref. [17], for ^{122}Sn Ref. [18], and for ^{124}Sn Ref. [19].

[c] Reference [21].

TABLE II. Total $B(E2)\uparrow$ strengths in the Sn isotopes between 2 and 4 MeV. The experimental data are compared with the results of QPM calculations.

Isotope	$\Sigma_{2<E<4\ \mathrm{MeV}} B(E2)\uparrow$ $(e^2\ \mathrm{fm}^4)$ $(\gamma,\ \gamma')$	$\Sigma_{2<E<4\ \mathrm{MeV}} B(E2)\uparrow$ $(e^2\ \mathrm{fm}^4)$ QPM
^{116}Sn[a]	143 (19)	203
^{118}Sn	151 (20)	226
^{120}Sn	283 (57)	240
^{122}Sn	236 (37)	237
^{124}Sn[a]	309 (45)	217

[a]See Ref. [8].

be underestimated and $\Gamma_{0,(n,n'\gamma)}$ will be overestimated. For the strong $E1$ transitions to the two-phonon states, the discrepancy between both values has another origin: strong transitions correspond to short lifetimes, which are difficult to be measured accurately with the Doppler shift attenuation method applied in the $(n,n'\gamma)$ experiments.

Several 2^+ states are observed in each of the Sn nuclei. In Table II and the bottom part of Fig. 2, the observed $B(E2)\uparrow$ quadrupole excitation probabilities between 2 and 4 MeV in the different Sn isotopes are presented. This energy interval was chosen to eliminate the influence of the dominating 2_1^+ state. The total $E2$ strength in this energy region is about an order of magnitude weaker than the 2_1^+ state and is nearly constant throughout the Sn isotopic chain. The $B(E2)\uparrow$ values of the 2_1^+ state in each of the Sn nuclei has also been investigated in Coulomb excitation experiments [23]. The agreement with our results for ^{118}Sn and ^{124}Sn is excellent. For ^{116}Sn and ^{122}Sn the $B(E2)\uparrow$ values differ by 15% and for ^{120}Sn by 20%. However, these transitions are located in a region of the NRF spectrum where the background increases highly due to nonresonant scattering of the photons, resulting in the statistical uncertainties of 10 to 15 % mentioned in Table I. Thus also for these last nuclei we can consider that the agreement between the NRF and Coulomb excitation results is fair.

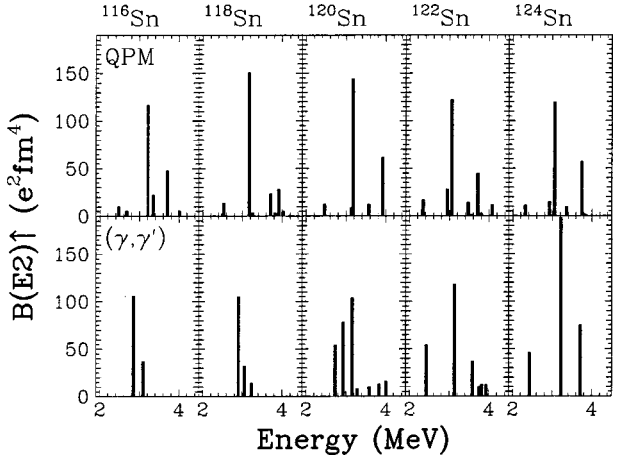

FIG. 2. Comparison between the calculated (top) and experimentally observed (bottom) $B(E2)\uparrow$ strengths for 2^+ states between 2 and 4 MeV in the Sn isotopes.

IV. DISCUSSION

The properties of the 2^+ states from the present experimental studies, including the results for ^{116,124}Sn [8] are compared in Table II and Fig. 2 with the corresponding results from the QPM calculation. This model has already proven to be successful in describing the properties of one-phonon and multiphonon states in a variety of other nuclei [7,24,25]. It provides complementary information about the microscopic wave functions of the excited states which is not available in an experimental analysis.

The QPM formalism and general technical details of its application to the description of the properties of low-lying states in spherical nuclei can be found in Ref. [26]. In the present calculations excited states in even-even nuclei with angular momentum J and projection M are described by a wave function including different one-, two-, and three-phonon configurations:

$$\Psi^{\nu}_{JM}=\left\{\sum_{\alpha} S^{\nu}_{\alpha}(J)Q^{+}_{\alpha}+\sum_{\alpha\beta}\frac{D^{\nu}_{\alpha\beta}(J)[Q^{+}_{\alpha}\otimes Q^{+}_{\beta}]_{JM}}{\sqrt{1+\delta_{\alpha,\beta}}}+\sum_{\substack{\alpha\beta\gamma\\ I}}\frac{T^{\nu}_{\alpha\beta\gamma}(J)[[Q^{+}_{\alpha}\otimes Q^{+}_{\beta}]_{I}\otimes Q^{+}_{\gamma}]_{JM}}{\sqrt{1+\delta_{\alpha,\beta}+\delta_{\alpha,\gamma}+\delta_{\beta,\gamma}+2\,\delta_{\alpha,\beta,\gamma}}}\right\}|\rangle_{\mathrm{ph}}. \tag{1}$$

In this expression $|\rangle_{\mathrm{ph}}$ is the wave function of the 0^+ ground state, the phonon vacuum. The Greek characters α, β, and γ represent the phonon's indexes (λ,μ,i) with λ the multipolarity, μ its projection and $i=1,\ 2,\ 3,\ldots$ labeling whether the phonon with quantum numbers λ^{π} has the lowest, next to lowest, etc. excitation energy. Multiphonon configurations are constructed by folding the phonon operators. The phonons $Q^{+}_{\lambda\mu i}$ (treated as quasibosons) are composed of many two-quasiparticle components of a definite spin and parity λ^{π}:

$$Q^{+}_{\lambda\mu i}=\frac{1}{2}\sum_{\tau}^{n,p}\sum_{\substack{jj'\\ mm'}}\{\psi^{\lambda i}_{jj'}C^{\lambda\mu}_{jmj'm'}\alpha^{+}_{jm}\alpha^{+}_{j'm'}-(-1)^{\lambda-\mu}\varphi^{\lambda i}_{jj'}C^{\lambda-\mu}_{j'm'jm}\alpha_{j'm'}\alpha_{jm}\}, \tag{2}$$

where α^{+}_{jm} (α_{jm}) is a creation (annihilation) operator of a quasiparticle on a level of an average field with quantum numbers $j\equiv|n,l,j\rangle$ and projection m. The energy spectrum of the one-phonon excitations and their internal fermion structure is obtained by solving the quasiparticle-RPA equations. The spectrum of excited states described by the wave function in Eq. (1) is obtained by a diagonalization of the model Hamiltonian in the space of these states. The diagonalization also yields the contribution of one-phonon and multiphonon configurations, with respective coefficients $S^{\nu}(J)$, $D^{\nu}(J)$, and $T^{\nu}(J)$, to the structure of each $\nu=1,2,3,\ldots$, excited state with quantum numbers J^{π}.

According to a spherical vibrator model, the first 2_1^+ state is highly collective with a large $B(E2)\uparrow$ strength of about 2000 e^2 fm^4. The QPM wave function [Eq. (1)] of this state

consists for 96–99 % of the first quadrupole RPA phonon. Its transition charge density is characterized by a surface peak typical for collective low-lying states and is in a good agreement with the experimental one [27]. The QPM predicts for each Sn isotope another, however less collective, one-phonon 2^+ state with an energy between 3.0 and 3.2 MeV and a $B(E2)\uparrow$ strength of about 120–150 e^2 fm^4. The other 2^+ phonons with an energy less than 5 MeV are noncollective (i.e., are practically pure two-quasiparticle configurations). Thus, their properties mainly depend on the average field used in the calculation and not on the strength of the residual interaction.

The $B(E2)$ strength distribution over the low-lying 2^+ excited states is determined by the one-phonon components of the wave function, Eq. (1). It is compared to the experimental results in Table II and Fig. 2. The contribution of the two-phonon components to the reduced transition probability for direct excitation of the 2^+ states from the ground state does not exceed a few percent of the total $E2$ one-phonon strength for the energy interval between 2 and 4 MeV. Nevertheless, two-phonon configurations cannot be neglected in the description of the characteristics of the low-lying 2^+ states since their role is essential to achieve the correct $E2$-strength fragmentation. A small admixture of one-phonon components stemming from the isoscalar giant quadrupole resonance does not change appreciably the total $E2$ strength in this energy region. The general agreement of the QPM predictions with experimental findings in both the $E2$-strength fragmentation and the total amount of strength is rather good.

V. CONCLUSIONS

Besides the 1^- two-phonon states, we observed in the even mass tin isotopes in addition to the well-known collective 2_1^+ state several other 2^+ states of lower collectivity below 4 MeV. The $B(E2)\uparrow$-strength distribution is rather similar along the chain of the Sn isotopes. A QPM analysis of 2^+ states shows that one-phonon configurations in their wave functions are responsible for the total $B(E2)\uparrow$ strength while the admixtures of more complex configurations lead to a fragmentation of the strength.

ACKNOWLEDGMENTS

This work is part of the Research program of the Fund for Scientific Research-Flanders. The support by the Deutsche Forschungsgemeinschaft (DFG) under Contracts No. Kn 154-30 and Br 799/9-1 is gratefully acknowledged. V.Yu.P. acknowledges the support from the RFBR (Grant No. 96-15-96729) and the Research Council of the University Gent.

[1] S. C. Fultz, B. L. Berman, J. T. Caldwell, R. L. Bramblett, and M. A. Kelly, Phys. Rev. **168**, 1255 (1969).
[2] A. Lepretre, H. Beil, R. Bergère, P. Carlos, A. De Minac, A. Veyssière, and K. Kernbach, Nucl. Phys. **A219**, 39 (1976).
[3] A. Bohr and B. Mottelson, *Nuclear Structure* (Benjamin, New York, 1975), Vol. 2.
[4] P. O. Lipas, Nucl. Phys. **82**, 91 (1966).
[5] N. Pietralla, D. Belic, P. von Brentano, C. Fransen, R.-D. Herzberg, U. Kneissl, H. Maser, P. Matschinsky, A. Nord, T. Otsuka, H. H. Pitz, V. Werner, and I. Wiedenhöver, Phys. Rev. C **58**, 796 (1998).
[6] N. Pietralla, C. Fransen, D. Belic, P. von Brentano, C. Friessner, U. Kneissl, A. Linnemann, A. Nord, H. H. Pitz, T. Otsuka, I. Schneider, V. Werner, and I. Wiedenhöver, Phys. Rev. Lett. **83**, 1303 (1999).
[7] M. Pignanelli, N. Blasi, J. A. Bordewijk, R. de Leo, M. N. Harakeh, M. A. Hofstee, S. Micheletti, R. Perrino, V. Yu. Ponomarev, V. G. Soloviev, A. Sushkov, and S. Y. van der Werf, Nucl. Phys. **A559**, 1 (1993).
[8] K. Govaert, L. Govor, E. Jacobs, D. De Frenne, W. Mondalaers, K. Persyn, M.-L. Yoneama, U. Kneissl, J. Margraf, H. H. Pitz, K. Huber, S. Lindenstruth, R. Stock, K. Heyde, A. Vdovin, and V. Yu. Ponomarev, Phys. Lett. B **335**, 113 (1994).
[9] J. Bryssinck, L. Govor, D. Belic, F. Bauwens, O. Beck, P. von Brentano, D. De Frenne, T. Eckert, C. Fransen, K. Govaert, R.-D. Herzberg, E. Jacobs, U. Kneissl, H. Maser, A. Nord, N. Pietralla, H. H. Pitz, V. Yu. Ponomarev, and V. Werner, Phys. Rev. C **59**, 1930 (1999).
[10] L. I. Govor, A. M. Demidov, O. K. Zhuravlev, I. V. Mikhailov, and E. Yu. Shkuratova, Sov. J. Nucl. Phys. **54**, 196 (1991).
[11] U. Kneissl, H. H. Pitz, and A. Zilges, Prog. Part. Nucl. Phys. **37**, 349 (1996).
[12] H. Maser, S. Lindenstruth, I. Bauske, O. Beck, P. von Brentano, T. Eckert, H. Friedrichs, R. D. Heil, R.-D. Herzberg, A. Jung, U. Kneissl, J. Margraf, N. Pietralla, H. H. Pitz, C. Wesselborg, and A. Zilges, Phys. Rev. C **53**, 2749 (1996).
[13] B. Schlitt, U. Maier, H. Friedrichs, S. Albers, I. Bauske, P. von Brentano, R. D. Heil, R.-D. Herzberg, U. Kneissl, J. Margraf, H. H. Pitz, C. Wesselborg, and A. Zilges, Nucl. Instrum. Methods Phys. Res. A **337**, 416 (1994).
[14] K. Govaert, W. Mondalaers, E. Jacobs, D. De Frenne, K. Persyn, S. Pomme, M.-L. Yoneama, S. Lindenstruth, K. Huber, A. Jung, B. Starck, R. Stock, C. Wesselborg, R.-D. Heil, U. Kneissl, and H. H. Pitz, Nucl. Instrum. Methods Phys. Res. A **337**, 265 (1994).
[15] A. M. Demidov and I. V. Mikhailov, Topics At. Sci. Technol. Ser. Nucl. Const. **4**, 24 (1990).
[16] I. V. Mikhailov and A. M. Demidov, Bull. Acad. Sci. USSR, Phys. Ser. **53**, 69 (1989).
[17] A. M. Demidov and I. V. Mikhailov, Sov. J. Nucl. Phys. **55**, 481 (1992).
[18] A. M. Demidov and I. V. Mikhailov, Bull. Acad. Sci. USSR, Phys. Ser. **55**, 30 (1991).
[19] A. M. Demidov and I. V. Mikhailov, Bull. Acad. Sci. USSR, Phys. Ser. **54**, 41 (1990).
[20] J. Blachot and G. Marguier, Nucl. Data Sheets **73**, 81 (1994).
[21] S. Raman, T. A. Walkiewicz, S. Kahane, E. T. Jurney, J. Sa, Z.

Gacsi, J. L. Weil, K. Allaart, G. Bonsignori, and J. F. Shriner, Jr., Phys. Rev. C **43**, 521 (1991).
[22] Z. Gacsi and S. Raman, Phys. Rev. C **49**, 2792 (1994).
[23] R. H. Spear, A. Baxter, S. Burnett, and C. Miller, Aust. J. Phys. **42**, 41 (1989); N.-G. Jonsson, A. Bäcklin, J. Kantele, R. Julin, M. Luontama, and A. Passoja, Nucl. Phys. **A371**, 333 (1981); A. Bäcklin and N. G. Jonsson, *ibid.* **A351**, 490 (1981).
[24] R. K. J. Sandor, H. P. Blok, U. Garg, M. N. Harakeh, C. W. de Jager, Y. Yu. Ponomarev, A. I. Vdovin, and H. de Vries, Nucl. Phys. **A535**, 669 (1991).
[25] V. Yu. Ponomarev, M. Pignanelli, N. Blasi, A. Bontempi, J. A. Bordewijk, R. de Leo, C. Graw, M. N. Harakeh, D. Hofer, M. A. Hofstee, S. Micheletti, R. Perrino, and S. Y. van der Werf, Nucl. Phys. **A601**, 1 (1996).
[26] V. Yu. Ponomarev, Ch. Stoyanov, N. Tsoneva, and M. Grinberg, Nucl. Phys. **A635**, 470 (1998).
[27] J. E. Wise, J. P. Connelly, F. W. Hersman, J. H. Heisenberg, W. Kim, F. W. Leushner, S. A. Fayans, A. P. Platonov, E. E. Saperstein, and V. Yu. Ponomarev, Phys. Rev. C **45**, 2701 (1992).